2

Propagation in a cold plasma

2.1 The Appleton–Hartree equation

As mentioned in Section 1.1, for a really cold plasma ($T_\alpha \to 0$) the condition (1.1) is no longer valid and all the theory developed in Chapter 1 breaks down. Thus when speaking about cold plasma we will assume that its temperature is so low that the contributions of thermal and relativistic corrections to ϵ_{ij} (the terms ϵ_{ij}^t and ϵ_{ij}^r in (1.78)) to the process of wave propagation are small when compared with the contribution of ϵ_{ij}^0, but at the same time this temperature is high enough for condition (1.1) to remain valid. This definition of a cold plasma obviously depends on the type of waves under consideration. The cold plasma approximation allows us to write the dispersion equation for various waves in a particularly simple form and it has been widely used for the analysis of waves (in particular, whistler-mode) in the magnetosphere. Some results of plasma wave theory based on this approximation will be recalled below.

Neglecting the contribution of the terms ϵ_{ij}^t and ϵ_{ij}^r in (1.78) we can assume $\epsilon_{ij} = \epsilon_{ij}^0$ in the expressions for A, B and C defined by (1.43)–(1.45) and rewrite them as:

$$A = A_0 \equiv S \sin^2\theta + P\cos^2\theta, \tag{2.1}$$

$$B = B_0 \equiv RL\sin^2\theta + PS(1+\cos^2\theta), \tag{2.2}$$

$$C = C_0 \equiv PRL, \tag{2.3}$$

where index $_0$ indicates that the corresponding coefficients refer to a cold plasma approximation; S, R, L and P are the same as in (1.79). When deriving (2.1)–(2.3) we took into account only the contribution of electrons to the process of wave propagation, as was done when deriving (1.78).

In view of (2.1)–(2.3) the cold plasma solution of (1.42) can be written as:

$$N_0^2 = (B_0 \pm F)/2A_0, \tag{2.4}$$

where

$$F^2 = (RL - PS)^2 \sin^4\theta + 4P^2D^2\cos^2\theta. \tag{2.5}$$

From (2.4) it follows that not more than two types of waves can propagate in a cold plasma in a fixed direction. When ω is real then N_0 can be either real ($N_0^2 > 0$) or imaginary (but not complex), which follows from the fact that $F^2 \geq 0$. If N_0 is imaginary then the wave cannot propagate; if N_0 is real then the wave propagates without damping or growth.

After some rearrangement equation (2.4) can be rewritten as (Ratcliffe, 1959; Holter & Kildal, 1973):

$$N_0^2 = 1 - \frac{2X(1-X)}{2(1-X) - Y^2\sin^2\theta \pm Y\sqrt{Y^2\sin^4\theta + 4(1-X)^2\cos^2\theta}}. \tag{2.6}$$

This equation is commonly known as the Appleton–Hartree equation (for a discussion about this name see Rawer & Suchy, 1976). It can be further simplified for some limiting values of θ, X or Y. For example, for $\theta = 0$ and $X > 1$ it reduces to:

$$N_0^2 = 1 - \frac{X}{1 \mp Y} \tag{2.7}$$

(for $X < 1$ the signs before Y in (2.7) are to be reversed; for $X = 1$ the cold plasma approximation is no longer valid unless θ is equal to zero: see equations (5.2)–(5.5)). In what follows we will be interested in the solution corresponding to the upper sign in (2.6) in the frequency range $Y > 1$. In this case (2.7) further reduces to:

$$N_0^2 = N_{0\parallel}^2 \equiv 1 + \frac{X}{Y-1}. \tag{2.8}$$

Waves described by equation (2.8) are known as whistler-mode waves (the origin of this name will be discussed later in this chapter) and they will be discussed in detail in the rest of the book.

Some attempts have been made to generalize (2.8) for finite θ avoiding, at the same time, returning to the full Appleton–Hartree equation. This was done by imposing the following conditions:

$$\left.\begin{aligned} Y^2\sin^2\theta &\ll 2|1-X| \\ Y^2\sin^4\theta &\ll 4(1-X)^2\cos^2\theta \end{aligned}\right\} \tag{2.9}$$

known as the quasi-longitudinal approximation (e.g. Stix, 1962).

Conditions (2.9) seem to allow us to neglect the contribution of the terms proportional to $\sin^2\theta$ and $\sin^4\theta$ in equation (2.6) and simplify it to the equation similar to (2.8) but with Y replaced by $Y\cos\theta$ (e.g. Stix, 1962; Helliwell, 1965). However, as was first pointed out by Budden (1983), if we neglect the term proportional to $\sin^2\theta$ in equation (2.6) we should also assume $\cos^2\theta = 1$, as the terms proportional to $(1 - \cos^2\theta)$ have the same order of magnitude as those proportional to $\sin^2\theta$ unless

$$X \gg 1. \tag{2.10}$$

As a result, we can generalize (2.8) for finite θ only when condition (2.10) is valid. When both conditions (2.9) and (2.10) are valid, equation (2.6) for whistler-mode waves is simplified to:

$$N_0^2 = N_{0d}^2 \equiv \nu \tilde{N}_{0d}^2, \tag{2.11}$$

where $\nu = \Pi^2/\Omega^2$, $\tilde{N}_{0d} = Y/\sqrt{Y\cos\theta - 1}$. This equation is the generalization of equation (2.8) for finite θ provided conditions (2.9) and (2.10) are valid. The plots of $\tilde{N}_{0d}$ versus θ for $Y^{-1} = 0.2$, 0.4 and 0.6 are shown in Fig. 2.1. As follows from this figure, $\tilde{N}_{0d} > 2$ and increases when θ increases. Minimum $\tilde{N}_{0d} = 2$ is achieved when $\theta = 0$ and $Y^{-1} = 0.5$. This means that condition (2.10) can in fact be replaced by a less stringent condition:

$$\nu \gg 0.5. \tag{2.12}$$

In view of (2.10), conditions (2.9) are satisfied for a wide range of θ except in the immediate vicinity of $\pi/2$. However, equation (2.11) predicts wave propagation ($N_0^2 > 0$) only when

$$\theta < \arccos Y^{-1} \equiv \theta_{R0}. \tag{2.13}$$

Moreover, if θ is close to θ_{R0} then $N_0^2 \to \infty$ and ϵ_{ij}^t in (1.78) can no longer be neglected when compared with ϵ_{ij}^0. For these θ the cold plasma approximation breaks down altogether.

Also, equation (2.8) can be generalized for $\theta \neq 0$ when condition (2.10) (or (2.12)) is not necessarily valid but

$$|\theta| \ll 1. \tag{2.14}$$

In view of (2.14) we can expand $\sin\theta$ and $\cos\theta$ in (2.6) in a Taylor series with respect to θ and write this equation for whistler-mode waves as:

$$N_0^2 = N_{0\|}^2(1 + a_0\theta^2), \tag{2.15}$$

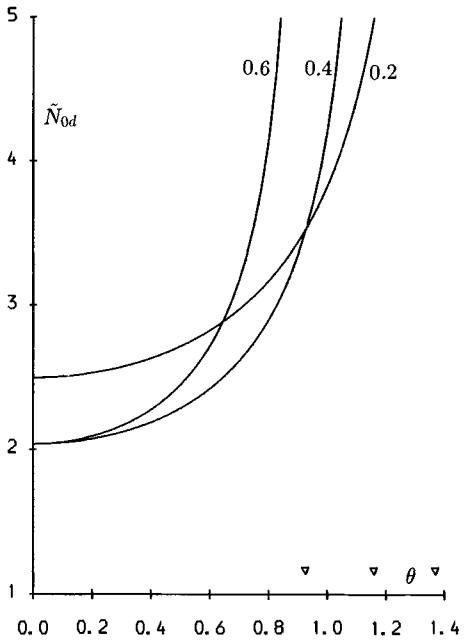

Fig. 2.1 Plots of $\tilde{N}_{0d} = Y/\sqrt{Y\cos\theta - 1}$ versus θ, the wave normal angle (in radians), for $Y^{-1} = 0.2$, 0.4 and 0.6 (figures near the curves). $\triangledown$ near the θ axis indicate $\theta = \theta_{R0} = \arccos Y^{-1}$ for these Y^{-1}.

where

$$a_0 = \frac{XY}{2(X-1)(Y-1)}, \tag{2.16}$$

and $N_{0\|}$ is defined by (2.8).

Equation (2.15) is valid when

$$|a_0\theta^2| \ll 1. \tag{2.17}$$

Condition (2.17) is hereafter considered as the quasi-longitudinal approximation for the plasma with arbitrary electron density, i.e. when condition (2.10) (or (2.12)) is not necessarily valid.

Remembering (2.16), condition (2.17) is always violated when X is close to 1 unless $\theta = 0$. Hence, one should be cautious when applying (2.8) to the interpretation of actual wave data at these X. When $X > 1$ then $a_0 > 0$ in the whistler-mode frequency range. Hence, N_0 determined by (2.15) increases with increasing θ as was the case with dense plasma (see equation (2.11) and Fig. 2.1).

Alternatively, if conditions (2.9) and (2.10) (or (2.12)) are valid but we

are interested in retaining terms of the order of X^{-1} (or ν^{-1}), then equation (2.6) for whistler-mode waves is simplified to:

$$N_0^2 = N_{0d}^2(1 + \tilde{a}_c\nu^{-1}), \tag{2.18}$$

where

$$\tilde{a}_c = \frac{Y^2\cos^2\theta - 4Y\cos\theta + Y^2 + 2}{2Y^2(Y\cos\theta - 1)}, \tag{2.19}$$

and N_{0d} is defined by (2.11); when deriving (2.18) we assumed that

$$|a_c| \equiv |\tilde{a}_c\nu^{-1}| \ll 1. \tag{2.20}$$

The term a_c describes the correction to N_{0d} due to the finite electron density. If $\theta = 0$ then $\tilde{a}_c$ simplifies to $(Y-1)/Y^2$. The same expression could be obtained from equation (2.8).

Remembering (1.150) and (1.151), equation (2.18) can be generalized so that the contribution of ions is taken into account as well (Sazhin, 1990a):

$$N_0^2 = N_{0d}^2(1 + \tilde{a}_c\nu^{-1} + \tilde{a}_r r), \tag{2.21}$$

where $\tilde{a}_r = -\tilde{a}_c Y^2$, $r = \sum_\alpha \Pi_\alpha^2/\Pi^2$ (the summation is assumed over all ion species; in the case when only the contribution of protons is to be taken into account then $r = m_e/m_p$, m_p is the proton mass),

$$|\tilde{a}_r r| \ll 1. \tag{2.22}$$

Plots of $\tilde{a}_c$ versus θ and $\tilde{a}_r$ versus θ are shown in Fig. 2.2, for the same Y^{-1} as in Fig. 2.1. As follows from Fig. 2.2, $\tilde{a}_c > 0$ and increases with increasing θ. The maximal value of $\tilde{a}_c = 0.25$ is achieved at $\theta = 0$ and $Y^{-1} = 0.5$. In contrast to $\tilde{a}_c$, $\tilde{a}_r < 0$ and $|\tilde{a}_r|$ increases with increasing θ and/or Y^{-1}. In fact the contribution of ions tends to compensate for the contribution of finite electron density.

In a similar way to (2.21) we can generalize the expression for the resonance cone angle defined by (2.13) so that the contribution of finite electron density and ions could be taken into account (Sazhin, 1989a):

$$\theta_R = \theta_{R0} - \frac{\sqrt{Y^2-1}}{2Y^2}\nu^{-1} + \frac{\sqrt{Y^2-1}}{2}r. \tag{2.23}$$

N^2 for whistler-mode waves is positive when $\theta < \theta_R$, and $N \to \infty$ when $\theta \to \theta_R$.

As can be seen from (2.23) the contribution of ions tends to compensate for the contribution of finite electron density as was the case in (2.21).

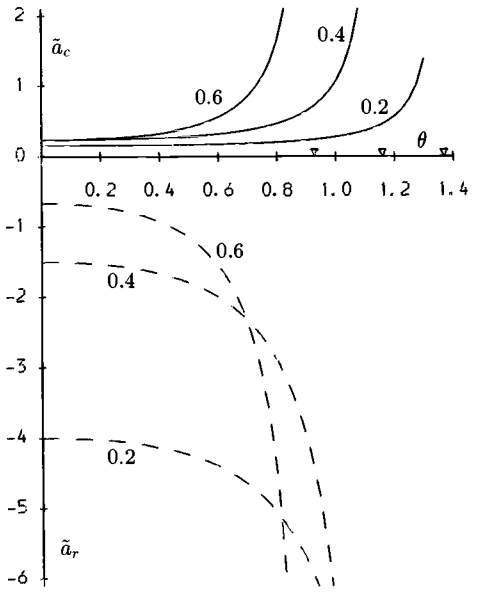

Fig. 2.2 Plots of $\tilde{a}_c$ (see equation (2.19)) versus θ (solid) and $\tilde{a}_r = -Y^2\tilde{a}_c$ versus θ (dashed) for $Y^{-1} = 0.2$, 0.4 and 0.6 (curves indicated). $\triangledown$ near the θ axis indicate $\theta = \theta_{R0} \equiv \arccos Y^{-1}$ for these Y^{-1}.

When deriving (2.23) it was assumed that the corrections to θ_{R0} due to finite ν^{-1} and r are small. In the general case of arbitrary ν but with the contribution of ions neglected, the expression for the resonance cone angle θ_R can be obtained by equating the denominator of (2.6) to zero. As a result we obtain:

$$\theta_R = \arcsin\sqrt{\frac{P(1-Y^2)}{\nu Y^4}}. \tag{2.24}$$

In the whistler-mode frequency range ($Y > 1$) expression (2.24) is defined when $P < 0$, i.e. when the wave frequency is below the electron plasma frequency.

Expressions (2.8), (2.11), (2.15), (2.21), (2.23) and (2.24) will be used for the analysis of different limiting cases of whistler-mode propagation throughout the whole book. Meanwhile we will consider another parameter which is also important for the analysis of the properties of whistler-mode waves, namely the group velocity.

2.2 Whistler-mode group velocity

The solution of a cold plasma dispersion equation referring to whistler-mode waves and discussed in the previous section allowed us to determine the wave refractive index N and, correspondingly, the wave phase velocity $v_{ph} = \omega/k = c/N$. However, this does not necessarily coincide with the velocity of energy flow. Without discussing details of the mathematical analysis of wave packet propagation (see Brillouin, 1960; Suchy, 1972; Anderson, Askne & Lisak, 1975, 1976; Tanaka, Fujiwara & Ikegami, 1986; Tanaka, 1989; Xu & Yeh, 1990, for details) we can refer only to the final result of this analysis. Namely, when the waves are not strongly damped or amplified and the dispersion is not large then the wave packet, or, in other words, cluster of wave energy, propagates with the so-called group velocity determined by the following equation:

$$\mathbf{v}_g = \mathrm{d}\omega/\mathrm{d}\mathbf{k}. \tag{2.25}$$

This result holds true for most cases of whistler-mode propagation in the magnetosphere and will be assumed throughout the whole book.

We begin our analysis with the simplest case of parallel whistler-mode propagation in a dense plasma when N_0 is determined by the equation (2.8) taken in the limit (2.10) (or (2.12)), or by equation (2.11) taken in the limit $\theta = 0$. After some straightforward algebra we obtain the following expression for v_g (which in this case is directed along $\mathbf{N}$, i.e. parallel to the magnetic field):

$$v_g = v_{g0} \equiv \frac{2c(Y-1)^{3/2}}{\sqrt{\nu}Y^2}, \tag{2.26}$$

where ν is the same as in (2.11).

As follows from (2.26), v_g approaches zero when either $\omega \to 0$ ($Y \to \infty$) or $\omega \to \Omega$ ($Y \to 1$). (Strictly speaking v_g never reaches zero in either case as the contribution of ions and finite electron temperature cannot be neglected when $\omega \to 0$ and $\omega \to \Omega$ respectively: see Section 4.3). Hence, we can expect v_g to be maximal for an intermediate frequency determined from the condition:

$$\mathrm{d}v_g/\mathrm{d}Y = 0. \tag{2.27}$$

In view of (2.26) condition (2.27) can be rewritten as:

$$\frac{c(Y-1)^{1/2}}{2\sqrt{\nu}Y^3}(4-Y) = 0. \tag{2.28}$$

The obvious solution of (2.28) in the range $1 < Y < \infty$ is $Y = 4$ or $\omega = 0.25\Omega$. Having substituted this solution into (2.26) we obtain:

$$v_g = v_{g\max} \equiv \frac{3\sqrt{3}c}{8\sqrt{\nu}} \approx \frac{0.65c}{\sqrt{\nu}}. \tag{2.29}$$

This maximal whistler-mode group velocity is manifested in the minimal group delay time for whistler-mode waves propagating from one hemisphere to another, as can be seen from whistler dynamic spectra shown in Fig. I. This group delay time can be calculated from the equation:

$$t_g = \int_{-s_{\text{ion}}}^{+s_{\text{ion}}} \frac{\mathrm{d}s}{v_g}, \tag{2.30}$$

where the integration is assumed along the magnetic field line between the opposite hemispheres; in the simplest model of a cold dense plasma v_g is defined by (2.26). As follows from (2.30) and (2.26) the main contribution to the integral in equation (2.30) comes from the part of the integration path where Ω is minimal, i.e. from the vicinity of the magnetospheric equator. Calculation of this integral for realistic models of electron distribution in the magnetosphere leads us to the result that t_g is minimal when $\omega \approx 0.4\Omega_{\text{eq}}$, where Ω_{eq} is the modulus of electron gyrofrequency at the magnetospheric equator (Carpenter & Smith, 1964; Park, 1972). Thus reading the frequency at which t_g is minimal, ω_n (nose frequency), from a whistler spectrogram (see e.g. Fig. I) we can determine the field line along which the whistler propagates. For given models of electron density distribution along the field lines and magnetic field (e.g. dipole field), t_g at the nose frequency depends on electron density at the magnetospheric equator (n_{eq}). Thus direct measurements of t_g allow us to estimate this density. Alternatively, measurements of ω_n at different moments of time allow us to get information about the motion of magnetic field tubes in the magnetosphere, and eventually about the large-scale electric field E_0 therein. Practical diagnostics of these parameters with the help of whistlers appears to be not so straightforward. Some particular problems related to this diagnostics will be discussed in Section 9.1. Meanwhile we shall consider other properties of v_g in some more detail.

Using (2.21), expression (2.26) for v_g can be generalized so that the contribution of finite electron density and ions can be taken into account (Sazhin, Smith & Sazhina, 1990):

$$v_g = v_{g0}(1 + \tilde{b}_c\nu^{-1} + \tilde{b}_r r), \tag{2.31}$$

where v_{g0} is determined by (2.26),

$$\tilde{b}_c = \frac{(4-3Y)(Y-1)}{2Y^3}, \tag{2.32}$$

$$\tilde{b}_r = \frac{1-Y}{2}. \tag{2.33}$$

When deriving equation (2.31) it was assumed that:

$$\left.\begin{array}{l} |\tilde{b}_c \nu^{-1}| \ll 1 \\ |\tilde{b}_r r| \ll 1 \end{array}\right\} \tag{2.34}$$

(cf. conditions (2.20) and (2.22)).

As follows from (2.31) the contribution of ions cannot be neglected when Y is sufficiently large. Thus, this equation is not valid for these Y either (see the discussion following (2.26)). $\tilde{b}_c < 0$ when $Y^{-1} < 0.75$ and $\tilde{b}_c > 0$ when $0.75 < Y^{-1} < 1$. $|\tilde{b}_c|$ achieves its maximum $|\tilde{b}_c|_{\max} \approx 0.19$ when $Y^{-1} = 6/(14+\sqrt{52}) \approx 0.28$. $|\tilde{b}_r|$ monotonically decreases when Y^{-1} increases.

When $\theta \neq 0$ the direction of $\mathbf{v}_g$ does not, in general, coincide with the direction of $\mathbf{k}$. In this case $\mathbf{v}_g$ can be presented in the form (Stix, 1962):

$$\mathbf{v}_g = \mathbf{e}_k \frac{\partial \omega}{\partial |\mathbf{k}|} + \mathbf{e}_\theta \frac{1}{|\mathbf{k}|} \frac{\partial \omega}{\partial \theta}, \tag{2.35}$$

where $\mathbf{e}_k$ and $\mathbf{e}_\theta$ are the unit vectors in the directions parallel and perpendicular to $\mathbf{k}$ respectively, but coplanar with $\mathbf{v}_g$ and $\mathbf{k}$. The angles are hereafter assumed positive if measured in a clockwise direction.

Restricting our analysis to whistler-mode propagation in a cold dense plasma and neglecting the contribution of ions, we can write the dispersion equation in the form (2.11). This equation can be solved with respect to ω and written as:

$$\omega = -\frac{c^2 k^2 \Omega \cos\theta}{c^2 k^2 + \Pi^2}. \tag{2.36}$$

In view of (2.36), equation (2.35) can be rewritten as:

$$\mathbf{v}_g = v_{gk}\mathbf{e}_k + v_{g\theta}\mathbf{e}_\theta, \tag{2.37}$$

where

$$v_{gk} = \frac{2c(Y\cos\theta - 1)^{3/2}}{\sqrt{\nu} Y^2 \cos\theta}, \tag{2.38}$$

$$v_{g\theta} = -\frac{c\sqrt{Y\cos\theta - 1}}{\sqrt{\nu Y}} \tan\theta. \tag{2.39}$$

Alternatively the expression for $\mathbf{v}_g$ can be presented as:

$$\mathbf{v}_g = v_{g\parallel}\mathbf{e}_\parallel + v_{g\perp}\mathbf{e}_\perp, \tag{2.40}$$

where

$$v_{g\parallel} = \frac{c\sqrt{Y\cos\theta - 1}(Y\cos^2\theta - 2\cos\theta + Y)}{\sqrt{\nu}Y^2\cos\theta}, \tag{2.41}$$

$$v_{g\perp} = -\frac{c\sqrt{Y\cos\theta - 1}\sin\theta(Y\cos\theta - 2)}{\sqrt{\nu}Y\cos\theta}, \tag{2.42}$$

$\mathbf{e}_\parallel$ is the unit vector in the direction parallel to the magnetic field (z axis), and $\mathbf{e}_\perp$ is the unit vector in the x direction (as in Chapter 1, $\mathbf{k}$ is supposed to lie in the (x, z) plane; $0 \leq \theta < \pi/2$).

From (2.38) and (2.39) or (2.41) and (2.42) we obtain the expression for the absolute value of v_g:

$$|v_g| = \frac{c\tilde{v}_g}{\sqrt{\nu}}, \tag{2.43}$$

where

$$\tilde{v}_g = \frac{\sqrt{Y\cos\theta - 1}}{Y^2\cos\theta}\sqrt{4(Y\cos\theta - 1)^2 + Y^2\sin^2\theta}. \tag{2.44}$$

Plots of $\tilde{v}_g$ versus θ are shown in Fig. 2.3 for the same Y^{-1} as in Figs. 2.1 and 2.2. As follows from this figure, $\tilde{v}_g$ decreases with increasing θ for any particular value of Y^{-1} until the cold plasma approximation breaks down for θ close to θ_{R0}.

As follows from (2.42), $v_{g\perp} = 0$ when

$$\theta = \theta_{G0} \equiv \arccos(2/Y), \tag{2.45}$$

which means that the whistler-mode group velocity for this particular θ is directed parallel to the magnetic field. This property of whistler-mode propagation seems to have been first noticed by Gendrin (1960) and so the angle θ_{G0} is known as the Gendrin angle. This angle is obviously defined only for $\omega < \Omega/2$. At $\omega > \Omega/2$, as well as at $\omega < \Omega/2$ and $\theta_{G0} < \theta < \theta_{R0}$ (see (2.13)), $v_{g\perp} < 0$ which means that the component of whistler-mode group velocity perpendicular to the external magnetic field is oppositely directed with respect to the corresponding component of $\mathbf{k}$ ($k_\perp$). When θ approaches θ_{R0}, then $|v_g| \to 0$. Whistler-mode waves in a cold dense electron plasma cannot propagate at $\theta > \theta_{R0}$. In the case when the contribution of finite electron density and ions is to be taken into account, θ_{R0} should be replaced by θ_R defined by (2.23) or (2.24). If $\theta < \theta_{R0}$ then $v_{g\parallel} > 0$ and so $v_{g\parallel}$ is parallel to $k_\parallel$.

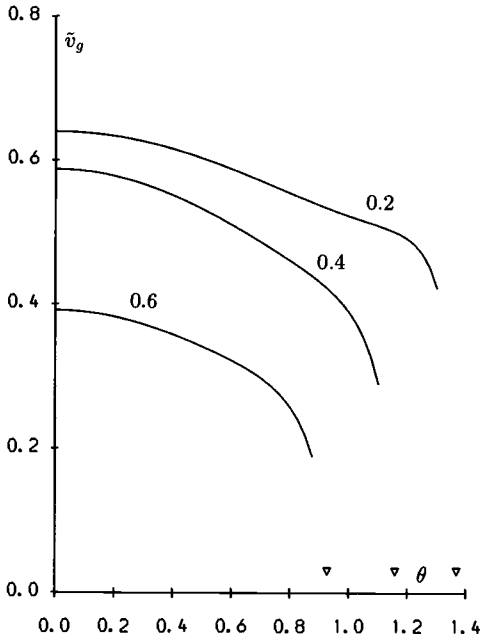

Fig. 2.3 Plots of $\tilde{v}_g$ (see equation (2.44)) versus θ for $Y^{-1} = 0.2$, 0.4 and 0.6 (curves indicated). $\triangledown$ near the θ axis indicate $\theta = \theta_{R0} \equiv \arccos Y^{-1}$ for these Y^{-1}.

In many practically important cases of whistler-mode propagation we are interested not only in the value of $|\mathbf{v}_g|$ but also in the direction of $\mathbf{v}_g$ with respect to $\mathbf{k}$ or $\mathbf{B}_0$. The corresponding angles between $\mathbf{k}$ and $\mathbf{v}_g$ (measured from $\mathbf{k}$ to $\mathbf{v}_g$) (θ_g) or between $\mathbf{B}_0$ and $\mathbf{v}_g$ ($\psi = \theta + \theta_g$) can be determined from the relatively simple equations which will be considered below. In particular, from (2.35) it follows that:

$$\tan\theta_g = \frac{1}{|\mathbf{k}|}\frac{\partial\omega}{\partial\theta} \Big/ \frac{\partial\omega}{\partial|\mathbf{k}|} = -\frac{1}{N}\frac{\partial N}{\partial\theta}. \tag{2.46}$$

Expression (2.46) allows a rather simple geometrical interpretation: $\mathbf{v}_g$ is perpendicular to the surface $N(\theta)$. When deriving this expression we made no assumptions about the wave dispersion equation and so this expression can be applied to any type of plasma wave, not necessarily whistler-mode waves.

Having substituted (2.11) into (2.46) we obtain:

$$\theta_g = \theta_{g0} \equiv -\arctan\left[Y\sin\theta/(2(Y\cos\theta - 1))\right], \tag{2.47}$$

$$\psi = \psi_0 \equiv \theta - \arctan\left[Y\sin\theta/(2(Y\cos\theta - 1))\right]. \tag{2.48}$$

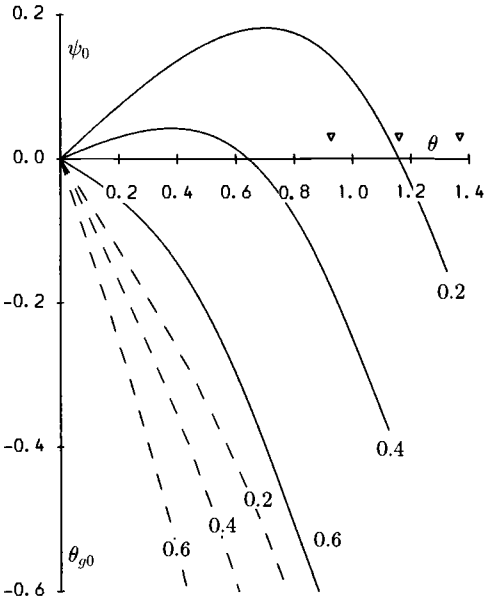

Fig. 2.4 Plots of θ_{g0} (see equation (2.47)) versus θ (dashed) and ψ_0 (see equation (2.48)) versus θ (solid) for $Y^{-1} = 0.2$, 0.4 and 0.6 (curves indicated). $\triangledown$ near the θ axis indicate $\theta = \theta_{R0} \equiv \arccos Y^{-1}$ for these Y^{-1}.

As follows from (2.48), $\psi_0 = \theta + \theta_{g0} = 0$ when $\theta = \theta_{G0}$ (see expression (2.45)) which agrees with the results of the analysis of (2.42). Also in agreement with the previous results we can see from (2.48) that $\psi_0 \leq 0$ when $1 < Y \leq 2$ or $Y > 2$ and $\theta \geq \theta_{G0}$, and $\psi_0 \geq 0$ when $Y > 2$ and $\theta \leq \theta_{G0}$. These properties of the angle ψ_0 follow from Fig. 2.4, where we show the plots ψ_0 versus θ and θ_{g0} versus θ. As follows from this figure, θ_{g0} is always negative and $|\theta_{g0}|$ increases with increasing θ and Y^{-1}. As to ψ_0, its behaviour appears to be different for $Y^{-1} > 0.5$ and $Y^{-1} < 0.5$. In the first case it is always negative and $|\psi_0|$ increases when θ and/or Y^{-1} increase. In the second case it is positive and first increases with increasing θ then reaches its maximum and then decreases with increasing θ reaching $\psi_0 = 0$ at $\theta = \theta_{G0}$. If $\theta > \theta_{G0}$ then $\psi_0 < 0$. If $\theta = 0$ then $\psi_0 = 0$. If θ approaches $\theta_{R0} = \arccos Y^{-1}$ then $\theta_{g0} \to \pi/2$ and $\psi_0 \to \theta - \pi/2$. Thus for the resonance cone whistler-mode wave normal angle $\mathbf{v}_g \perp \mathbf{N}$.

In the limit $Y \gg 2$ expression (2.46) is simplified to:

$$\theta_{g0} = -\arctan(0.5 \tan\theta). \tag{2.49}$$

In view of (2.48) and (2.49) we obtain:

$$\tan\psi_0 = \frac{\tan\theta + \tan\theta_{g0}}{1 - \tan\theta\tan\theta_{g0}} = \frac{0.5\tan\theta}{1 + 0.5\tan^2\theta}. \tag{2.50}$$

As follows from (2.50), $\psi_0 \to 0$ when $\theta \to 0$ or when $\theta \to \pi/2$. Thus we can expect that ψ_0 should attain its maximal value for an intermediate value of θ. The value of θ at which ψ_0 is maximal follows from the equation:

$$\frac{\mathrm{d}\tan\psi_0}{\mathrm{d}\tan\theta} = 0. \tag{2.51}$$

In view of (2.50) this equation has a solution:

$$\theta = \theta_{s0} \equiv \arctan\sqrt{2} = 54.74^\circ = 0.955\,\mathrm{rad}. \tag{2.52}$$

Substituting (2.52) into (2.50) we obtain:

$$\psi(\theta_{s0}) = \psi_{s0} \equiv \arctan 0.25\sqrt{2} = 19.47^\circ = 0.340\,\mathrm{rad}. \tag{2.53}$$

That the whistler-mode group velocity at low frequencies does not deviate from the magnetic field by more than about 19.5° was first discovered by Storey (1953). Hence, the angle ψ_{s0} is known as the Storey angle.

The concept of the Storey angle can be generalized to the case when Y is above but not well above 2, when θ_{s0} and ψ_{s0} are determined by the following equations:

$$\theta_{s0} \equiv \arccos\left[Y^{-1} + \frac{\sqrt{1 - Y^{-2}}}{\sqrt{3}}\right], \tag{2.54}$$

$$\psi_{s0} \equiv \theta_{s0} - \arctan\left[\frac{Y\sin\theta_{s0}}{2(Y\cos\theta_{s0} - 1)}\right]. \tag{2.55}$$

The plots of θ_{s0} versus Y^{-1} and ψ_{s0} versus Y^{-1} are shown in Fig. 2.5. In the same figure we have shown for comparison the plot $-\psi_{R0} = -(\theta_{R0} - \pi/2) = -(\arccos Y^{-1} - \pi/2)$ versus Y^{-1}. The latter plot describes the direction of whistler-mode group velocity at $\theta = \theta_{R0}$. All the plots are shown only for $Y^{-1} \leq 0.5$ when θ_{s0} and ψ_{s0} are determined ($\cos\theta_{s0} \leq 1$).

As follows from Fig. 2.5, ψ_{s0} and θ_{s0} are maximal when $Y^{-1} \to 0$, while ψ_{R0} is close to zero for these Y^{-1}. An increase of Y^{-1} is accompanied by a decrease in both ψ_{s0} and θ_{s0} until they reach zero at $Y^{-1} = 0.5$. The values of $-\psi_{R0}$ increase almost linearly with increasing Y^{-1} in the same frequency range. At a certain Y^{-1} slightly below 0.2, $\psi_{s0} = -\psi_{R0}$. This means that the deviation of the direction of whistler-mode group velocity from the direction of magnetic field $\mathbf{B}_0$ is mainly controlled by ψ_{s0} at $Y^{-1} < 0.2$ and by ψ_{R0}

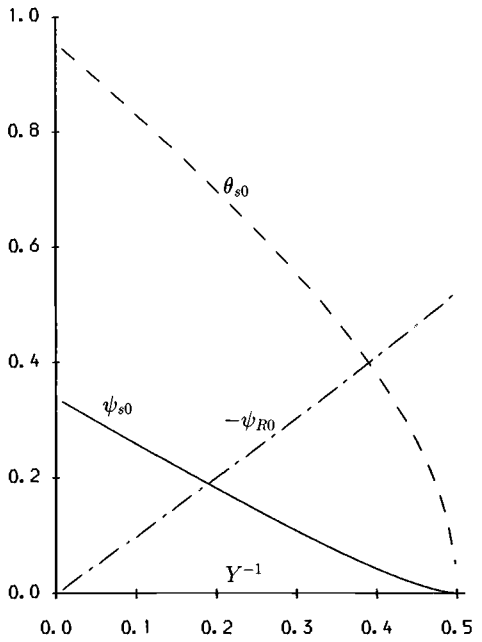

Fig. 2.5 Plots of θ_{s0} (see equation (2.54)) versus Y^{-1} (dashed), ψ_{s0} (see equation (2.55)) versus Y^{-1} (solid) and $-\psi_{R0} \equiv \pi/2 - \arccos Y^{-1}$ versus Y^{-1} (dashed–dotted).

at $Y^{-1} > 0.2$. Note that the values of ψ_{s0} determined by (2.55) correspond to the maxima of ψ_0 in Fig. 2.4.

In the case when finite electron density and the contribution of ions is taken into account, (2.48) can be generalized to:

$$\psi = \psi_0 + \tilde{\Delta}_c \nu^{-1} + \tilde{\Delta}_r r, \tag{2.56}$$

where

$$\tilde{\Delta}_c = \frac{(Y^2 - 2 + 2Y\cos\theta - Y^2\cos^2\theta)\sin\theta}{Y(-Y^2 - 4 + 8Y\cos\theta - 3Y^2\cos^2\theta)}, \tag{2.57}$$

$$\tilde{\Delta}_r = -Y^2\tilde{\Delta}_c. \tag{2.58}$$

Plots of $\tilde{\Delta}_c$ versus θ and $\tilde{\Delta}_r$ versus θ are shown in Fig. 2.6. As follows from this figure, $\tilde{\Delta}_c$ is always negative and $|\tilde{\Delta}_c|$ increases with increasing θ and/or Y^{-1}. $\tilde{\Delta}_r$ is always positive and increases with increasing θ and/or Y^{-1}. Thus the effects of finite electron density and the contribution of ions tend to compensate for each other as was the case in evaluating N_0 (see equation (2.21) and Fig. 2.2).

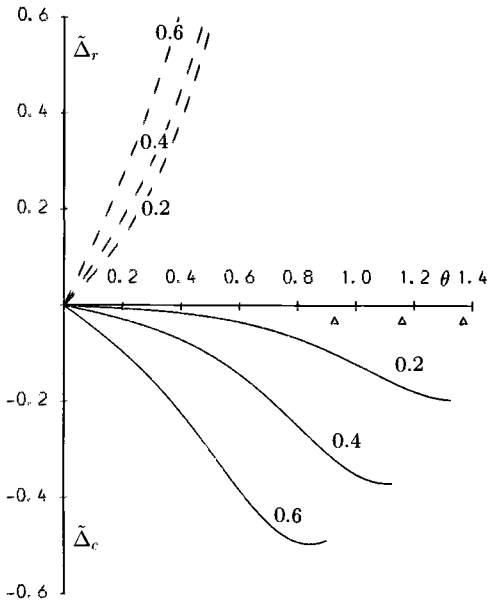

Fig. 2.6 Plots of $\tilde{\Delta}_c$ (see equation (2.57)) versus θ (solid) and $\tilde{\Delta}_r$ (see equation (2.58)) versus θ (dashed) for $Y^{-1} = 0.2$, 0.4 and 0.6 (curves indicated). $\triangle$ near the θ axis indicate $\theta = \theta_{R0} \equiv \arccos Y^{-1}$ for these Y^{-1}.

In view of (2.56) expressions (2.52) and (2.53) are generalized to (Sazhin, 1990a):

$$\theta_s = \theta_{s0} + \Delta\theta_s, \tag{2.59}$$

$$\psi_s = \psi_{s0} + \Delta\psi_s, \tag{2.60}$$

where

$$\Delta\theta_s = \Delta\tilde{\theta}_{cs}\nu^{-1} + \Delta\tilde{\theta}_{rs}r, \tag{2.61}$$

$$\Delta\tilde{\theta}_{cs} = \frac{(Y^2-1)(5Y\cos\theta_{s0} - 8)}{9Y^3\sin\theta_{s0}(1 - Y\cos\theta_{s0})}, \tag{2.62}$$

$$\Delta\tilde{\theta}_{rs} = -\Delta\tilde{\theta}_{cs}Y^2, \tag{2.63}$$

$$\Delta\psi_s = \tilde{\Delta}_{cs}\nu^{-1} + \tilde{\Delta}_{rs}r, \tag{2.64}$$

$$\tilde{\Delta}_{cs} = \frac{(Y^2 - 2 + 2Y\cos\theta_{s0} - Y^2\cos^2_{s0}\theta)\sin\theta_{s0}}{Y(-Y^2 - 4 + 8Y\cos\theta_{s0} - 3Y^2\cos^2\theta_{s0})}, \tag{2.65}$$

$$\tilde{\Delta}_{rs} = -Y^2\tilde{\Delta}_{cs}. \tag{2.66}$$

θ_{s0} and ψ_{s0} are the same as in (2.54) and (2.55).

In a similar way to (2.59), finite electron density and ion effects change the Gendrin angle defined by (2.45) so that the whistler-mode group velocity is directed along the magnetic field when (Sazhin, 1988b, 1990a):

$$\theta_G = \theta_{G0} + \Delta\theta_G, \tag{2.67}$$

where

$$\left.\begin{aligned} \Delta\theta_G &= \Delta\tilde{\theta}_{cG}\nu^{-1} + \Delta\tilde{\theta}_{rG}r \\ \Delta\tilde{\theta}_{cG} &= (2-Y^2)/(Y^2\sqrt{Y^2-4}) \\ \Delta\tilde{\theta}_{rG} &= -(2-Y^2)/\sqrt{Y^2-4} \end{aligned}\right\}. \tag{2.68}$$

As was the case with θ_R (see equation (2.23)) the corrections to θ_{G0} due to the contribution of finite electron density and the effect of ions tend to compensate each other.

The corrections to θ_R due to the contribution of finite electron density and ions determined by (2.23) result in the corresponding corrections to $\psi_R = \theta_R - \pi/2$. The corrections to the angles θ_{s0}, θ_{G0} and ψ_{s0} due to finite electron density and contribution of ions will be considered in more detail in Chapters 5 and 6 where we compare them with the corresponding corrections due to finite electron temperature and anisotropy.

2.3 Whistler-mode polarization

Whistler-mode dispersion and group velocity considered in the previous sections are important parameters for the study of the propagation of these waves in any realistic, and, in particular, magnetospheric plasma. However, they give us no information about the internal structure of the waves (polarization) and the physical background of their propagation. None of these aspects of whistler-mode theory seems to be of minor importance. Knowledge of whistler-mode polarization is essential for the study of the interaction of these waves with energetic electrons or for the determination of their wave normal angle based on the measurements of wave field components (see e.g. Sazhin, Walker & Woolliscroft, 1990a). Analysis of the physical background of whistler-mode propagation allows us to understand the process of wave propagation not in terms of the formal solution of the corresponding wave dispersion equation but rather in terms of the energy exchange between electric and magnetic fields of the wave and the electron current. A good feeling for this process would also contribute to a clearer understanding of the physical background of the process of whistler-mode electron interaction in general. Whistler-mode polarization in a cold plasma will be considered